Chinese Journal of Polymer Science Vol. 27, No. 3, (2009), 1–8

Chinese Journal of Polymer Science

THE ASSOCIATION OF LIVING POLYSTYRYLLITHIUM IN BENZENE*

Jun-fang Li, Shi-zhong Luo, Wei-dong He and Guang-zhao Zhang**

Department of Chemical Physics, Department of Polymer Science and Engineering The University of Science and Technology of China, Hefei 230026, China

Chi Wu

Department of Chemistry, The Chinese University of Hong Kong. Shatin. N. T., Hong Kong, China

Abstract The effects of the chain length, active end group and concentration on the association of living polystyryllithium (PS^-Li^+) chains in benzene were examined by a combination of static and dynamic laser light scattering in a cuvette equipped with a high-vacuum stopcock. The results show that long PS^-Li^+ chains ($M_w > 1 \times 10^4$) usually form dimers in the solution. In contrast, shorter PS^-Li^+ chains exhibit two relaxation modes, where the fast mode is related to the translational diffusion of the living chain dimers. The end capping of the living chain with bulky 1,1-diphenylethene (DPE) leads to an intensity increase of the slow mode, indicating that the slow mode is not due to the chain aggregates but to the long-range density fluctuation induced by weak electrostatic dipole-dipole interaction between ionic pairs at the chain ends.

Keywords: Light scattering; Anionic polymerization; Aggregate.

INTRODUCTION

Organolithium has been used to initiate living anionic polymerization for synthesizing narrowly distributed homopolymer chains or block copolymer chains with desired chain architectures for decades. It is recognized that the state of the organolithium has great effect on the chain initiation and growth. However, the mechanism is not clear. It has been reported that two to six organolithium initiator molecules could associate together in non-polar solvents such as benzene, hexane, cyclohexane and heptane[1–5]. On the other hand, some studies revealed that two and four short living polymer chains with one anionic end group could also associate during the polymerization[6–11]. The association can be examined by scattering technique[12, 13]. The dynamic laser light scattering and small angle neutron scattering (SANS) experiments by Fetters *et al*.[14] indicated that the living chains associated into unknown structures larger than −100 nm, which were attributed to the formation of worm-like micelles with a skeletal bond made of alternative carbon and lithium. Stellbrimk *et al*.[15–17] also reported that living anionic polymer chains formed such large structures.

In terms of the understanding of linear polymer chains in a good solvent, one can not imagine that the ionic pair at one end of each living polymer chain could associate and form such large structures. Considering that the solutions previously studied with living polymer chains were directly collected from the vacuum line with only a glass frit to filter out large fragments of the break-seals, the large structures were attributed to large dust particles[18]. Recently, Allgaier *et al.*[19, 20] improved the experiment by using a combination of a vacuum line and a dry box to clarify the solution of living polymer chains. The solution was sealed with a Young® stopcock to avoid air contamination. They used time-resolved ^{1}H-NMR and SANS to follow the polymerization of butadiene initiated by *tert*-butyl lithium in *d*-heptane. To their surprise, they also observed large structures in the initial

* This work is supported by the Hong Kong Special Administration Region Earmarked Grants (CUHK4036/05P, 2160269), the Chinese Academy of Sciences Special Grant (No. KJCX2-SW-H14), China Postdoctoral Science Foundation (No. 20070420727) and the National Natural Science Foundation Project (No. 20574065).

** Corresponding author: Guang-zhao Zhang (张广照), E-mail: gzzhang@ustc.edu.cn

Received February 29, 2008; Revised March 9, 2008; Accepted March 19, 2008

stage of polymerization. Moreover, the apparent association number decreased with the polymerization degree. So far, the origin of such large structures is still questionable.

In the present study, we have clarified the monomer and initiator solutions with a Millipore filter inside a dry box and used a cuvette equipped with a high vacuum stopcock for laser light scattering (LLS) experiments, so that we can rule out any possible contamination of dust particles. By use of a combination of static and dynamic LLS, we have examined the effects of the chain length, active end group, concentration and solvent quality on the association of living polystyryllithium (PS^-Li^+) chains in benzene. We attempted to understand the origin of the aggregates in the solution.

EXPERIMENTAL

Materials

sec-Butyllithium in *n*-hexane/cyclohexane (1.3 mol/L), *n*-butyllithium in *n*-hexane (2.79 mol/L) dibutylmagnesium[$Mg(bu)_2$ 1.0 mol/L] in heptane and 1,1-diphenylethene (DPE) were purchased from Aldrich. DPE was transferred into a flask sealed with a Young® stopcock on the high vacuum line after its reaction with *n*-butyllithium for 4 h. Styrene was distilled under reduced pressure after it was washed with aqueous solution of sodium hydroxide for three times and several times with water. After being stirred with CaH_2 at 60°C for 4 h, styrene was transferred into dibutylmagnesium and stood on a high-vacuum line (10^{-5} Torr) until it turned slightly yellow. Anhydrous styrene was obtained by collecting the medium fraction under the high vacuum into a flask sealed with a Young® stopcock. Benzene was stirred over with sulfate acid for a week, and then it was washed with aqueous solution of sodium hydroxide for three times and several times with water. Subsequently, it was stirred with CaH_2 at 60°C for 4 h, transferred into *n*-butyllithium and stood on vacuum line for more than one day[21]. It was then distilled into a flask with a Young® stopcock on a high-vacuum line. Such prepared reactants were moved from the high-vacuum line into a dry box (MBraun Unilab®, $O_2 < 0.1 \times 10^{-6}$ and $H_2O < 0.1 \times 10^{-6}$) just before use.

Anionic Polymerization of Styrene

Anionic polymerization of styrene was done in the dry box. All the solvent, styrene and initiations were mixed and then filtered into a specially prepared LLS cuvette equipped with a high vacuum stopcock by a 0.45 μm PTFE hydrophobic millipore filter which was cleaned by the living polymer solution. 11.0 mL *sec*-butyl lithium (1.3 mol/L) was mixed with 70.0 mL benzene in a flask with a protective stopcock. 5.0 mL styrene monomer was then slowly added into the flask at the room temperature. One portion of polystyryl lithium oligomers (PS^-Li^+) was taken for the further polymerization. The results are summarized in Table 1.

Table 1. LLS Characterization of PS samples

Sample	Styrene (mL)	Benzene (mL)	PS^-Li^+ (mmol)	$M_{n,cal} \times 10^{-3}$	$M_{n,GPC} \times 10^{-3}$	M_w/M_n	$R_{h,PS}$ (nm)	$k_BT/(6\pi\eta D)$ (nm) $R_{h,fast}$	$R_{h,slow}$	A_s
7-PSt	2.0	98	0.14	13.0	12.0	1.08	2.7	3.5	Non	
1-PSt	0.5	50	0.21	2.5	2.2	1.09	1.1	1.5	126	41%
3-PSt	2.0	100	0.42	4.7	4.6	1.04	1.9	2.2	101	27%
5-PSt	6.0	200	0.84	6.7	6.2	1.05	2.1	2.4	168	17%
6-PSt	2.5	50	0.21	11.0	11.0	1.01	2.2	2.9	Non	
2-PSt	4.0	75	1.3	2.8	2.7	1.03	1.2	1.6	112	39%
4-PSt	10.0	190	1.7	5.3	5.4	1.02	1.8	2.2	164	69%
8-PSt	2.0	37	0.11	16.0	17.0	1.01	3.1	4.0	Non	
9-PSt	0.60	29	0.026	21.0	23.0	1.01	3.8	6.2	Non	
10-PSt	0.45	29	0.010	41.0	41.0	1.02	5.0	7.0	Non	

A_s is the intensity contribution of the slow mode at the angle of 15°.

By varying initial concentrations of PS^-Li^+ and styrene, we prepared living anionic polystyryl lithium chains with different lengths (Sample 1, 3, 5, 6 in Table 1). The details are as follows: 10 mL PS^-Li^+ solution

(0.17 mol/L) was mixed with 390 mL benzene. The mixture was divided into four parts. Into each portion, a different amount of styrene was added. Note that each solution nearly contains the same concentration of active species. After polymerization at 20°C for 12 h, a small amount of the reaction mixture was taken out for the gel permeation chromatographer (GPC) and LLS analysis. GPC measurements were conducted on a Waters 150C using monodisperse polystyrene as the calibration standard and THF as the eluent with a flow rate of 1.0 mL/min. In LLS, we clarified a small amount (1–2 mL) of the solution directly into a dust-free LLS cuvette equipped with a Young® stopcock in the dry box by using a Millipore PTFE filter (0.45 μm). The polymer concentrations were kept below the overlap concentration (Φ^*) defined as $3M_w/(4\pi N_A R_g^3)$ to avoid possible chain entanglements, where N_A, M_w and R_g are the Avogadro constant, the weight-averaged molar mass and radius of gyration of polymer chains, respectively.

Laser Light Scattering

A commercial LLS spectrometer (ALV/DLS/SLS-5022F) equipped with a multi-digital time correlation (ALV5000) and a cylindrical 22 mW He-Ne laser (λ_0 = 632 nm, Uniphase) as the light source was used. In static LLS[22], we can obtain the weight-average molar mass (M_w) and the *z*-average root-mean square radius of gyration ($<R_g^2>^{1/2}$or written as $<R_g>$) of scattering objects in a dilute solution/dispersion from the angular and concentration dependence of the excess absolute scattering intensity (Rayleigh ratio $R_{vv}(q)$) as,

$$\frac{Kc}{R_{vv}(q)} \approx \frac{1}{M_w}(1+\frac{1}{3}<R_g^2>q^2)+2A_2c \tag{1}$$

where $K = 4\pi n^2(dn/dc)^2/(N_A\lambda_0^4)$ and $q = (4\pi n/\lambda_0)\sin(\theta/2)$ with N_A, dn/dc, n, and λ_0 being the Avogadro number, the specific refractive index increment, the solvent refractive index, and the wavelength of the light in a vacuum, respectively; and A_2 is the second virial coefficient. For short chains ($qR_g << 1$), the angular correction is not necessary. In this study, we used the scaling relation of $A_2 = 1.5 \times 10^{-2}M_w^{-0.276}$ to correct the concentration effect in Eq. (1)[23]. Such a scaling law is not exactly correct for very short chains. In the present study, it will not significantly affect the concentration correction because the solutions are in the dilute region.

In dynamic LLS[24], the Laplace inversion of each measured intensity-intensity-time correlation function $G^{(2)}(q, t)$ in the self-beating mode can lead to a characteristic relaxation time distribution $G(\tau)$. For a pure diffusive relaxation, τ is related to the translational diffusion coefficient D by $(1/\tau q^2)_{c\to 0,q\to 0} \to D$. In this case, $G(\tau)$ can be converted into a transitional diffusion coefficient distribution $G(D)$ or further to a hydrodynamic radius distribution $f(R_h)$ *via* the Stokes-Einstein equation, $R_h = (k_BT/6\pi\eta)/D$, where k_B, T and η are the Boltzmann constant, the absolute temperature, and the solvent viscosity, respectively. The cumulant analysis of $G^{(2)}(t)$ of a narrowly distributed sample can actually result in an accurate average characteristic relaxation time $<\tau>$ with a sufficient accuracy.

In the polymer solution, unimer, dimer and chain aggregates coexist[15–17]. Since the concentration of the aggregates is very low, we took the concentration of the individual chain as that of the solution. The apparent weight average molar mass ($M_{w,app}$) of the chains in the mixture can be calculate by the intensity contribution of the fast mode by DLS at different angles. Each peak in $G(\tau)$ corresponds to one kind of scattering species. The area (A) ratio of different peaks leads to the scattering intensity (I) ratio of different species. For a mixture of individual chains, the fast mode is related to the unimer, dimer and other small associates of chains, whereas the slow mode is related to the large aggregates, so we have

$$\frac{A_{chain}}{A_{aggregate}} = \frac{I_{chain}}{I_{aggregate}} \approx \frac{c_{chain}M_{w,chain}}{c_{aggregate}M_{w,aggregate}} \tag{2}$$

Define x as the relative weight, we know $\chi_{chain} = c_{chain}/(c_{chain} + c_{aggregate})$, and $\chi_{chain} + \chi_{aggregate} = 1$[25, 26]. On the basis of Eq. (2), we can obtain $M_{w,\,chain}$ and $\chi_{w,\,aggregate}M_{w,\,aggregate}$ from a combination of static and dynamic LLS results.

Since the molar mass of the aggregate is much large than the individual chain[27], the contribution of the fast mode to the intensity can be neglected, so χ_{chain} can be taken to be 1. After each LLS study, we terminated the living chains and measured the weight average molar mass of individual neutral chains ($M_{w,\ chain}$), so that we were able to calculate the association number ($M_{w,\ aggregate}/M_{w,\ chain}$).

RESULTS AND DISCUSSION

Figure 1 shows the typical GPC results of polystyrene samples prepared by anionic polymerization initiated with short living oligomeric PS^-Li^+ chains. Clearly, the samples are narrowly distributed. Thus, we can use M_w obtained from LLS to calculate the associate number of living chains. Here, due to the experimental uncertainty, the initiation efficiency ($M_{n,\ cal}/M_{n,\ GPC}$) of some samples are larger then 100%.

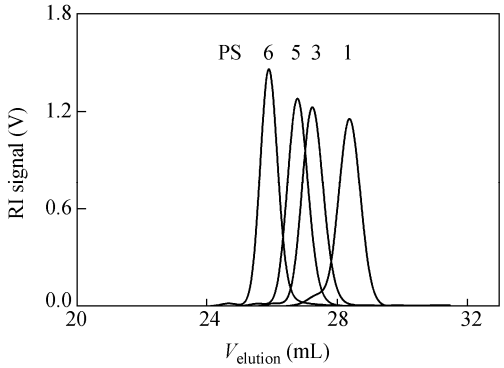

Fig. 1 Typical GPC curves of the terminated neutral PS samples

Figure 2 shows the intensity-intensity time correlation functions $G^{(2)}(q, t)$ of living anionic PS^-Li^+ chains and the end-terminated neutral PS chains (Sample 1) in benzene. In comparison with the latter, the former have a long tail in $G^{(2)}(q, t)$, indicating an additional slow relaxation. Such slow relaxation can be better viewed in terms of characteristic relaxation time distributions $G(\tau)$ in the inset. An additional peak with a longer relaxation time can be observed in $G(\tau)$.

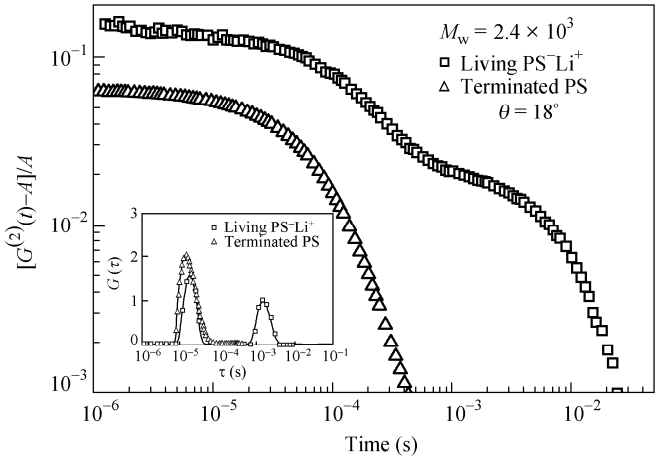

Fig. 2 Intensity-intensity time correlation functions of living PS^-Li^+ and the neutral PS chains in benzene with a concentration of 9.6×10^{-3} g/mL
The inset shows the corresponding characteristic relaxation time distributions $G(\tau)$.

Figure 3 shows the normalized intensity-intensity time correlation functions $G^{(2)}(q, t)$ of living PS^-Li^+

chains with different chain lengths in benzene and the corresponding characteristic relaxation time distributions $G(\tau)$, where the polymer concentrations were at (4.2 ± 0.3) μmol/mL. $G(\tau)$ is bimodal when living PS^-Li^+ chains are short ($M_w \leq \sim 1 \times 10^4$). Table 1 also shows that the solutions of Samples 1–5 have a slow mode. In addtion, the intensity contribution (the area under the peak related to the slow relaxation mode) decreases as the chain length increases. This is reasonable because the electrostatic interaction between the ends of long living PS^-Li^+ chains is weaker than that of shorter ones, or it would be easier for short ionic chains to form such worm-like structures because of much less loss of conformational entropy if the slow mode is caused by the large aggregate[28]. The slow mode even completely disappears when the molecular weight (M_w) of the living chains is above 1.14×10^4. Note that the fast mode is not due to individual chains or unimers. Using the corresponding terminated neutral PS chains as the references, we were able to estimate the average association number for the living PS^-Li^+ chains from the fast mode. The results are summarized in Table 2. The average association number for shorter living chain is 2.0 ± 0.2, in other words, most of the chains form dimers.

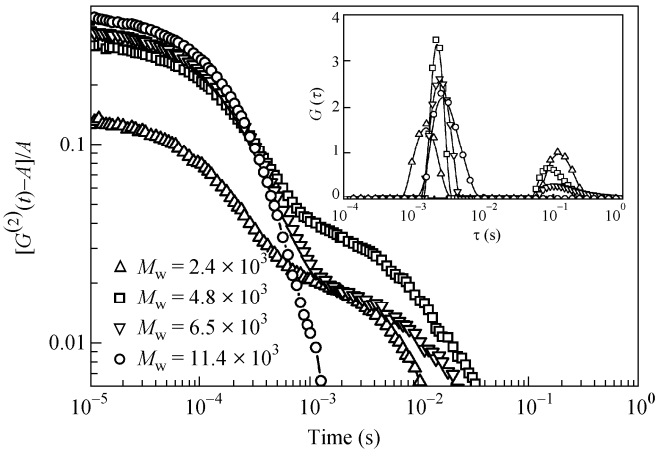

Fig. 3 Chain length dependence of intensity-intensity time correlation functions of living PS^-Li^+ chains in benzene

The concentrations of ionic end group are (4.2 ± 0.3) μmol/mL; The inset shows the characteristic relaxation time distributions $G(\tau)$.

Table 2. Average aggregation number (n) of living PS^-Li^+ chains with different lengths in benzene at 25°C

Sample	$M_{w,GPC}$	$M_{w,LLS}$*		n**
		Living chains	Terminated chains	
1-PS	2.4×10^3	4.1×10^3	1.9×10^3	2.1
2-PS	2.8×10^3	5.8×10^3	3.3×10^3	1.8
3-PS	4.8×10^3	1.0×10^4	4.9×10^3	2.1
4-PS	5.6×10^3	7.8×10^3	4.4×10^3	1.8
5-PS	6.5×10^3	1.1×10^4	5.5×10^3	2.0
6-PS	1.1×10^4	1.6×10^4	8.6×10^3	1.8
7-PS	1.3×10^4	2.5×10^4	1.4×10^4	1.8
8-PS	1.7×10^4	1.6×10^4	7.0×10^3	2.3
9-PS	2.3×10^4	3.6×10^4	1.8×10^4	2.0
10-PS	4.2×10^4	4.9×10^4	2.3×10^4	2.2

* For Samples 1–5, $M_{w,LLS}$ was estimated from the contribution of the fast mode on the basis of Eq. (1);
** $n = M_{w,living}/M_{w,terminated}$

Note that the weight concentrations of different living chains are fairly different though their molar concentrations are close. In other words, the solution of longer living chains is more concentrated. Accordingly, we have examined the concentration effect on the slow mode. The 3-PS^-Li^+ solution was divided into four parts.

Three of them were diluted with different amounts of dry benzene. Figure 4 shows their characteristic relaxation time distributions $G(\tau)$. Clearly, the positions of the fast and slow modes slightly change with the concentration. The quantitative results are summarized in Table 3. The slight increase of $<\tau>$ with dilution is due to the positive dynamic second virial coefficient (k_D) of polystyrene chains in benzene, which involves both the thermodynamic and hydrodynamic contributions. As the concentration increases, the motion of the chains becomes slower. Figure 4 and Table 3 clearly reveal that the absence of the slow mode in the solution of long living chains does not arise from the chain disassociation due to the dilution.

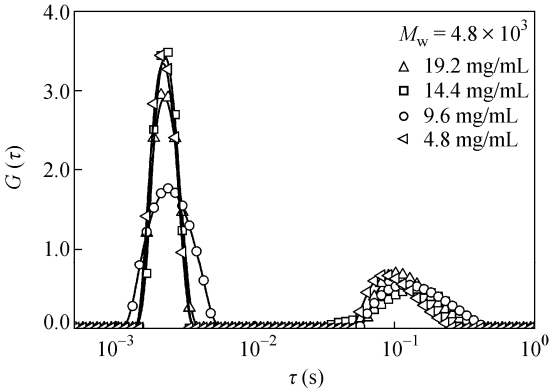

Fig. 4 Concentration dependence of characteristic relaxation time distributions $G(\tau)$ of living 3-PS^-Li^+ chains in benzene

Table 3. Effect of dilution on living 3-PS chains in benzene at 25°C

c_{PS} (g/mL)	$<\tau>_{fast}$ (s)	$<\tau>_{slow}$ (s)	A_{slow}
1.92×10^{-2}	2.79×10^{-4}	1.28×10^{-2}	27%
1.44×10^{-2}	2.91×10^{-4}	1.59×10^{-2}	31%
9.6×10^{-3}	2.92×10^{-4}	1.65×10^{-2}	28%
4.8×10^{-3}	3.17×10^{-4}	1.83×10^{-2}	31%

The slow mode has been attributed to micelle-like structure due to the clustering of living chains[18]. However, the living chains (M_w *ca.* 6000) have a length less than 15 nm even when they are fully stretched. The chains can not form a spherical cluster larger than 100 nm. It has also been suggested that the living chains form worm-like micelles with a skeletal bond made of alternative carbon and lithium[14–17, 28]. Since DPE organolithium end is bulky, it cannot initiate an anionic polymerization of DPE[29, 30]. If the slow mode is due to large aggregates or structures, the introduction of DPE end would destroy the large structures. Or, if the slow mode is not caused by the large structures but the dipole-dipole interaction of organolithium end, the DPE organolithium dipole is stronger than the PS^-Li^+ dipole, the presence of DPE would lead more chains association with a slow mode in the intensity-intensity time correlation functions $G^{(2)}(q, t)$. Therefore, we can examine whether the living chains form a worm-like structure by using DPE to change the structure of organolithium ends.

Figure 5 shows an additional slow mode for living 6-PS ($M_w = 1.1 \times 10^4$) chains when the chain ends are replaced by the DPE organolithium, and the inset shows only one relaxation mode in 6-PS or DPE capped 6-PS solutions. This indicates that the DPE end is soluble well in benzene. The effect of DPE on the slow mode becomes more obvious for even shorter living chains. Clearly, the slow mode in DPE capped living chains solution is not caused by the infusibility of DPE, but the living DPE organolithium or the dipole-dipole interaction.

Figure 6 shows that the presence of the DPE organolithium increases the intensity distribution of the slow mode when there are slow modes in the intensity-intensity time correlation functions $G^{(2)}(q, t)$ of living chains.

Figure 5 and Fig. 6 clearly exclude the existence of worm-like micelles with a skeletal bond made of alternative carbon and lithium. Since the DPE organolithium dipole is stronger than the PS^-Li^+ dipole, the slow mode will become have larger contribution with DPE organolithium then with normal organolithium. The results clearly show that the slow mode is related to the long-range density fluctuation induced by the dipole-dipole interaction.

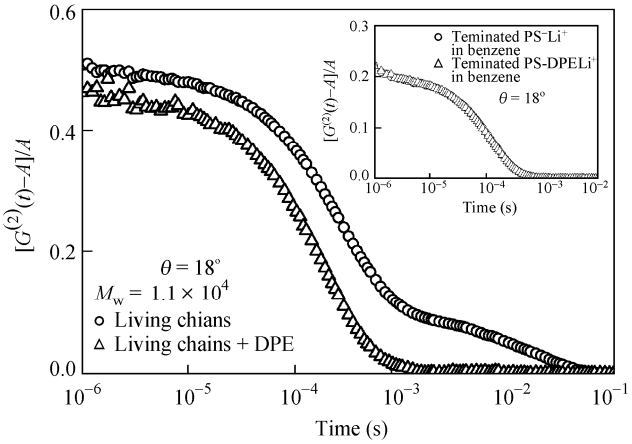

Fig. 5 Intensity-intensity time correlation functions of living 6-PS^-Li^+ chains with and without the end capping of DPE in benzene
The inset shows the intensity-intensity time correlation functions.

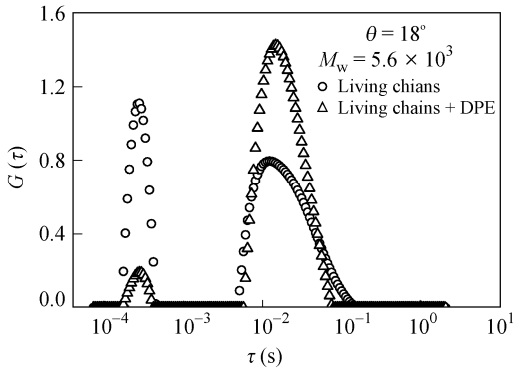

Fig. 6 Characteristic relaxation time distributions $G(\tau)$ of living 4-PS^-Li^+chains with and without the end capping of DPE in benzene

CONCLUSIONS

By use of a combination of static and dynamic laser light scattering, we have investigated the effects of the chain length, active end group and concentration on the association of living PS^-Li^+ chains in dilute solutions. The studies can lead to the following conclusion. Short living chains mainly exist as dimers in dilute solutions, presumably, due to the dipole-dipole interaction between the ionic pairs (S^-Li^+) at the end of living chains. The observed slow relaxation mode is not due to dust particles or micelle-like clusters of chains. Instead, it can be attributed to the long-range density fluctuation induced by the weak electrostatic dipole-dipole interactions.

REFERENCES

1 Brown, T.L., Dicherhoof, D.W. and Bafus, D.A., J. Am. Chem. Soc., 1962, 84: 1371

2 Brown, T.L., Ladd, J.A. and Newman, G., J. Orgmet. Chem., 1965, 3: 1
3 Margerison, D. and Newport, J.P., Trans. Faraday Soc., 1963, 59: 2062
4 Roovers, J.E.L. and Bywater, S., Macromolecules, 1975, 8: 251
5 Morton, M. and Fetters, L.J., Rubber Chem. Technol., 1975, A12: 359
6 Worsfold, D.J. and Bywater, S., Macromolecules, 1972, 5: 393
7 Nishimura, S.I., Furuike, T., Matsuoka, K., Maruyama, K., Nagata, K., Kurita, K., Nishi, N. and Tokura, S., Macromolecules, 1994, 27: 4876
8 Young, R.N., Quirk, R.P. and Fetters, L.J., Adv. Polym. Sci., 1984, 56: 1
9 Morton, M., Fetters, L.J. and Bostick, E.E., J. Polym .Sci. Part C, 1963, 1: 311
10 Morton, M. and Fetters, L.J., J. Polym. Sci. Part A, 1964, 2: 3331
11 Watanabe, H., Oishi, Y., Kanaya, T., Kaji, H. and Horii, F., Macromolecules, 2003, 36: 220
12 Morton, M., Fetters, L.J., Pett, R.A. and Meier, J.F., Macromolecules, 1970, 3: 327
13 Fetters, L.J. and Morton, M., Macromolecules, 1974, 7: 552
14 Fetters, L.J., Balsara, N.P., Huang, J.S., Joen, H.S., Almdal, K. and Lin, M.Y., Macromolecules, 1995, 28: 4996
15 Stellbrink, J., Willner, L., Jucknischke, O., Richter, D., Lindner, P., Fetters, L.J. and Huang, J.S., Macromolecules, 1998, 31: 4189
16 Stellbrink, J., Willner, L., Richter, D., Lindner, P., Fetters, L.J. and Huang, J.S., Macromolecules, 1999, 32: 5321
17 Stellbrink, J., Allgaier, J., Willner, L., Richter, D., Slawecki, T. and Fetters, L.J., Polymer, 2002, 43: 7101
18 Bywater, S., Macromolecules, 1998, 31: 6010
19 Niu, A.Z., Stellbrink, J., Allgaier, J., Willner, L., Richter, D., Koenig, B.W., Gondorf, M., Willbold, S., Fetters, L.J. and May, R.P., Macromol. Symp., 2004, 215: 1
20 Niu, A.Z., Stellbrink, J., Allgaier, J., Willner, L., Radulescu, A., Richter, D., Koenig, B.W., May, R.P. and Fetters, L.J., J. Chem. Phys., 2005, 122: 134906
21 Hadjichristidis, N., Iatrou, H., Pispas, S. and Pitsikalis, M., J. Polym. Sci. Part A, 2000, 38: 3211
22 Bene, B.J. and Pecora, R., "Dynamic Light Scattering", Plenum Press, New York, 1976
23 Li, J.B., Wan, Y.N., Xu, Z.D. and Mays, J.W., Macromolecules, 1995, 28: 5347; Nakamura, Y., Norisuye, T. and Teramoto, A., J. Polym. Sci. Part B, 1991, 29: 153
24 Chu, B. "Laser Scattering", 2nd ed., Academic Press, New York, 1991, p.84
25 Wu, C., Macromolecules, 1993, 26: 3821
26 Xu, Z., Yi, C., Cheng, R., Feng, L. and Wu, C., Acta. Polymerica Scinica(in Chinese), 2000, (6): 701
27 Cheng, H., Wu, C. and Winnik, M.A., Macromolecules, 2004, 37: 5127
28 Frischknecht, A.L. and Milner, S.T., J. Chem. Phys., 2001, 114: 1032
29 Laita, Z. and Szawarc, M., Macromolecules, 1969, 2: 412
30 Li, A. and Lu, Z., Science in China, Ser. B., 2007, 37(1): 31